Research Article | Vol. 9, No. 7 | 1 Jul 2018 | BIOMEDICAL OPTICS EXPRESS 3067

Biomedical Optics EXPRESS

Millisecond cellular labelling *in situ* with two-photon photoconversion

SHELDON J. J. KWOK,[1,2] YONGJAE JO,[3,4] HARVEY H. LIN,[1] MYUNGHWAN CHOI,[3,4,5] AND SEOK-HYUN YUN[1,2,6]

[1]*Harvard Medical School and Wellman Center for Photomedicine, Massachusetts General Hospital, 50 Blossom Street, Boston, MA 02114, USA*
[2]*Harvard-MIT Health Sciences and Technology, Massachusetts Institute of Technology, 77 Massachusetts Avenue, Cambridge, MA 02139, USA*
[3]*Department of Biomedical Engineering, Sungkyunkwan University, Suwon 16419, South Korea*
[4]*Center for Neuroscience Imaging Research, Institute for Basic Science, Suwon 16419, South Korea*
[5]*photomodulation@gmail.com*
[6]*syun@hms.harvard.edu*

Abstract: *In situ* labeling of cells within living biological tissues using photoconversion has provided valuable information on cellular physiology in their natural environments. However, current photoconvertible probes typically require seconds to minutes of light exposure, limiting their uses in rapid biological processes such as intracellular diffusion and circulating cells. Here, we report that two-photon photoconversion of cyanine-based dyes offers unprecedentedly rapid photoconversion down to millisecond timescales per cell. We demonstrate potential biological applications including measuring intracellular diffusion kinetics in a spinal nerve, labeling of rapidly flowing cells in a microfluidic channel, and photoconversion of a circulating cell *in vivo*.

OCIS codes: (160.2540) Fluorescent and luminescent materials; (020.4180) Multiphoton processes; (170.2520) Fluorescence microscopy.

References and links

1. T. Nagai, K. Ibata, E. S. Park, M. Kubota, K. Mikoshiba, and A. Miyawaki, "A variant of yellow fluorescent protein with fast and efficient maturation for cell-biological applications," Nat. Biotechnol. **20**(1), 87–90 (2002).
2. R. Weissleder and V. Ntziachristos, "Shedding light onto live molecular targets," Nat. Med. **9**(1), 123–128 (2003).
3. M. Choi, S. J. J. Kwok, and S. H. Yun, "In vivo fluorescence microscopy: lessons from observing cell behavior in their native environment," Physiology (Bethesda) **30**(1), 40–49 (2015).
4. G. H. Patterson and J. Lippincott-Schwartz, "A photoactivatable GFP for selective photolabeling of proteins and cells," Science **297**(5588), 1873–1877 (2002).
5. T. Matsuda, A. Miyawaki, and T. Nagai, "Direct measurement of protein dynamics inside cells using a rationally designed photoconvertible protein," Nat. Methods **5**(4), 339–345 (2008).
6. J. Konen, E. Summerbell, B. Dwivedi, K. Galior, Y. Hou, L. Rusnak, A. Chen, J. Saltz, W. Zhou, L. H. Boise, P. Vertino, L. Cooper, K. Salaita, J. Kowalski, and A. I. Marcus, "Image-guided genomics of phenotypically heterogeneous populations reveals vascular signalling during symbiotic collective cancer invasion," Nat. Commun. **8**, 15078 (2017).
7. R. Turcotte, J. W. Wu, and C. P. Lin, "Intravital multiphoton photoconversion with a cell membrane dye," J. Biophotonics **10**(2), 206–210 (2017).
8. T. Torcellan, H. R. Hampton, J. Bailey, M. Tomura, R. Brink, and T. Chtanova, "In vivo photolabeling of tumor-infiltrating cells reveals highly regulated egress of T-cell subsets from tumors," Proc. Natl. Acad. Sci. U.S.A. **114**(22), 5677–5682 (2017).
9. T. Chtanova, H. R. Hampton, L. A. Waterhouse, K. Wood, M. Tomura, Y. Miwa, C. R. Mackay, R. Brink, and T. G. Phan, "Real-time interactive two-photon photoconversion of recirculating lymphocytes for discontinuous cell tracking in live adult mice," J. Biophotonics **7**(6), 425–433 (2014).
10. A. L. Carlson, J. Fujisaki, J. Wu, J. M. Runnels, R. Turcotte, J. A. Spencer, C. L. Celso, D. T. Scadden, T. B. Strom, and C. P. Lin, "Tracking Single Cells in Live Animals Using A Photoconvertible Near-Infrared Cell Membrane Label," PLoS One **8**(8), e69257 (2013).
11. W. P. Dempsey, L. Georgieva, P. M. Helbling, A. Y. Sonay, T. V. Truong, M. Haffner, and P. Pantazis, "In vivo single-cell labeling by confined primed conversion," Nat. Methods **12**(7), 645–648 (2015).

#327504 https://doi.org/10.1364/BOE.9.003067
Journal © 2018 Received 9 Apr 2018; revised 23 May 2018; accepted 6 Jun 2018; published 11 Jun 2018

Biomedical Optics EXPRESS

12. D. A. Nedosekin, V. V. Verkhusha, A. V. Melerzanov, V. P. Zharov, and E. I. Galanzha, "In vivo photoswitchable flow cytometry for direct tracking of single circulating tumor cells," Chem. Biol. **21**(6), 792–801 (2014).
13. E. R. Pereira, D. Kedrin, G. Seano, O. Gautier, E. F. J. Meijer, D. Jones, S.-M. Chin, S. Kitahara, E. M. Bouta, J. Chang, E. Beech, H.-S. Jeong, M. C. Carroll, A. G. Taghian, and T. P. Padera, "Lymph node metastases can invade local blood vessels, exit the node, and colonize distant organs in mice," Science **359**(6382), 1403–1407 (2018).
14. S. J. J. Kwok, M. Choi, B. Bhayana, X. Zhang, C. Ran, and S.-H. Yun, "Two-photon excited photoconversion of cyanine-based dyes," Sci. Rep. **6**(1), 23866 (2016).
15. L. Dirix, K. Kennes, E. Fron, Z. Debyser, M. van der Auweraer, J. Hofkens, and S. Rocha, "Photoconversion of far-red organic dyes: implications for multi-color super-resolution imaging," ChemPhotoChem **2**(5), 433–441 (2018).
16. W. Watanabe, T. Shimada, S. Matsunaga, D. Kurihara, K. Fukui, S. Shin-Ichi Arimura, N. Tsutsumi, K. Isobe, and K. Itoh, "Single-organelle tracking by two-photon conversion," Opt. Express **15**(5), 2490–2498 (2007).
17. J. Crank, *The Mathematics of Diffusion* (Oxford University Press, 1979).
18. A. Vogel, J. Noack, G. Hüttman, and G. Paltauf, "Mechanisms of femtosecond laser nanosurgery of cells and tissues," Appl. Phys. B **81**(8), 1015–1047 (2005).
19. T. G. Gorgels and D. van Norren, "Ultraviolet and green light cause different types of damage in rat retina," Invest. Ophthalmol. Vis. Sci. **36**(5), 851–863 (1995).
20. M. L. Denton, M. S. Foltz, L. E. Estlack, D. J. Stolarski, G. D. Noojin, R. J. Thomas, D. Eikum, and B. A. Rockwell, "Damage Thresholds for Exposure to NIR and Blue Lasers in an In Vitro RPE Cell System," Invest. Ophthalmol. Vis. Sci. **47**(7), 3065–3073 (2006).
21. W. R. Zipfel, R. M. Williams, and W. W. Webb, "Nonlinear magic: multiphoton microscopy in the biosciences," Nat. Biotechnol. **21**(11), 1369–1377 (2003).
22. S. J. J. Kwok, M. Choi, B. Bhayana, X. Zhang, C. Ran, and S.-H. Yun, "Two-photon excited photoconversion of cyanine-based dyes," Sci. Rep. **6**(23866), 23866 (2016).
23. J. N. Post, K. A. Lidke, B. Rieger, and D. J. Arndt-Jovin, "One- and two-photon photoactivation of a paGFP-fusion protein in live Drosophila embryos," FEBS Lett. **579**(2), 325–330 (2005).
24. X. Kong, S. K. Mohanty, J. Stephens, J. T. Heale, V. Gomez-Godinez, L. Z. Shi, J.-S. Kim, K. Yokomori, and M. W. Berns, "Comparative analysis of different laser systems to study cellular responses to DNA damage in mammalian cells," Nucleic Acids Res. **37**(9), e68 (2009).
25. F. Persson, M. Lindén, C. Unoson, and J. Elf, "Extracting intracellular diffusive states and transition rates from single-molecule tracking data," Nat. Methods **10**(3), 265–269 (2013).
26. G. Katona, G. Szalay, P. Maák, A. Kaszás, M. Veress, D. Hillier, B. Chiovini, E. S. Vizi, B. Roska, and B. Rózsa, "Fast two-photon in vivo imaging with three-dimensional random-access scanning in large tissue volumes," Nat. Methods **9**(2), 201–208 (2012).
27. E. Papagiakoumou, A. Bègue, B. Leshem, O. Schwartz, B. M. Stell, J. Bradley, D. Oron, and V. Emiliani, "Functional patterned multiphoton excitation deep inside scattering tissue," Nat. Photonics **7**(4), 274–278 (2013).
28. E. Papagiakoumou, F. Anselmi, A. Bègue, V. de Sars, J. Glückstad, E. Y. Isacoff, and V. Emiliani, "Scanless two-photon excitation of channelrhodopsin-2," Nat. Methods **7**(10), 848–854 (2010).

1. Introduction

Advances in fluorescent probes for optical microscopy have revolutionized our understanding of complex biological systems [1–3]. In particular, photoconvertible probes enable *in situ* labeling of cells of interest by spatially localized light exposure, altering the emission spectrum of the probes [4,5]. The photoconverted cells of interest can be readily distinguished from non-photoconverted cells for *in vivo* tracking over large spatiotemporal scales or isolated for further *in vitro* molecular analyses [6–10].

Because of their unique capabilities, photoconvertible probes are widely utilized. However, most conventional photoconvertible probes have low photoconversion yields, usually requiring seconds to minutes of irradiation time to obtain detectable photoconversion [11,12]. The conversion speed can be improved by increasing irradiation intensity but is limited by the risk of phototoxicity. The requirement of poorly penetrating UV-blue irradiation also prevents efficient photoconversion of cells deep in scattering biological tissues. As a result, applications of photoconvertible proteins have mostly been applicable to nearly stationary or slowly moving cells, such as in 3D cell culture [6], tumors [8], and lymph nodes [13].

Recently, we have demonstrated that a number of cyanine-based fluorophores can undergo efficient two-photon photoconversion with applications for *in situ* cell labeling [14].

Biomedical Optics EXPRESS

The mechanism of photoconversion is thought to be an irreversible photoinduced chemical reaction [15]. Under two-photon excitation, these chemical fluorophores have significantly higher brightness and photoconversion yield compared to fluorescent protein-based approaches. Due to the nonlinearity in the absorption process, two-photon excitation enables photoconversion confined to the focal volume, enabling remote targeting of cells in three-dimensions [16]. Furthermore, nonlinearity in two-photon process enables faster photoconversion rates at lower overall fluence (i.e. energy density). These advantages led us to explore whether two-photon photoconversion could be used for *in situ* labeling of fast moving cells, such as flowing cells in blood circulation.

Here we report that two-photon photoconversion of cyanine-based dyes enables rapid labeling of a target cell *in situ*, down to millisecond timescales, faster than any previously reported process. We describe the theoretical background of rapid photoconversion mediated by the two-photon process and demonstrate potential biological applications, including measuring intracellular diffusion kinetics in a spinal nerve, and labelling of rapidly flowing cells in a microfluidic channel and in blood circulation *in vivo*.

2. Materials and methods

2.1 Microsocopy setup

A home-built two-photon microscope was used for imaging and photoconversion. The light source is a mode-locked Ti-Sapphire laser (MaiTai DeepSee eHP, Newport) delivering ~150 fs pulses at 80 MHz. The scanning unit consists of a polygon mirror for fast axis (x) and a galvanometer for slow axis (y), allowing frame rate of 30 Hz. Alternatively, a dual-axis galvanometer was used for axon diffusion studies to photoconvert only the selected region-of-interest in an axon fiber. One of the following water-immersion objectives was used: 40X 0.8 NA (Olympus), 20X 1.0 NA (Zeiss), or 16X 0.8 NA (Nikon). The polygon-based system is designed to have a fixed field-of-view (FOV) of 150 × 150 μm^2 with a 40X objective lens. The emitted light was detected by three photomultiplier tubes through dichroic mirrors and bandpass filters for the blue channel (400–485 nm), green channel (500–550 nm) and red channel (560–705 nm). Photoconversion experiments were conducted as previously described [14]. For measuring dye only, 3 µL of 3.75 mM SYTO62 (ThermoFisher Scientific) was mixed with 1 µL of 3 µm polystyrene beads ($10^{-4\%}$ v/v) and covered with a #1.5 coverslip for imaging. For measuring stained cells, HeLa cells were stained with SYTO62 and SYTO82 at 5 µM in cell media for 1 hour, and washed with PBS prior to imaging.

2.2 Diffusion measurements

Under anesthesia, the sciatic nerve was dissected and meninges was removed in physiologic saline. The nerve fibers were immersed in a 50 µM SYTO62 solution for 10 min. After washing with saline, the nerve fibers were mounted on a slide glass with #1.5 cover slip on top. The sample was then imaged at 4.1 mW and photoconverted at 22 mW for the duration of 6 s. For quantifying the diffusion of a dye alone, 1 mM SYTO62 was (5 µm in thickness) was photoconverted at 65 mW for 0.7 s and subsequently imaged at 25 mW (section 2.3). To quantify diffusion coefficients, the line intensity profile was fitted to the following one-dimensional diffusion formula [17]:

$$c(x,t) = \frac{1}{2} c_0 \left(erf \frac{h-x}{2\sqrt{Dt}} + erf \frac{h+x}{2\sqrt{Dt}} \right) \quad (1)$$

where $c(x,t)$ denotes the molecular concentration at position, x and time, t; c_0 is initial concentration; h is the half length of conversion segment, and D is a diffusion coefficient.

Biomedical Optics EXPRESS

2.3 Photoconversion in a microfluidic chamber

For demonstration of photoconversion of flowing cells, murine blood cells were first stained with SYTO62 by incubating 800 μL of blood cells with 10 μL of 5 mM SYTO62 for 1 hour. The cells were then fed through a microfluidic flow chamber (μ-Slide I0.8 Luer, ibidi) by a syringe pump (Legato 100, KD Scientific). For full frame photoconversion, the laser scanning area was kept fixed at 300 × 300 μm^2. For line scan photoconversion, the slow axis scanner (galvano-mirror) was turned off and cells were photoconverted as they flowed along the laser irradiation line scanning at ~15 kHz using a polygon scanner. To determine the reproducibility of line scan photoconversion, images were analyzed with MATLAB. The xt image was first integrated along the time axis to generate one-dimensional intensity traces for the red and green components. The time trace for the green was then fitted to the one-phase exponential curve to acquire conversion time.

2.4 In vivo photoconversion

For *in vivo* studies, we used 7-week-old male C57BL/6J mice (Jackson Laboratory). Under anesthesia with intraperitoneal injection of ketamine (90 mg/kg) and xylazine (9 mg/kg), the scalp was excised, and the skull was glued to a custom-made metal frame using a dental cement. Circular craniotomy of ~3 mm diameter was performed on the region of somatosensory cortex using a micro-drill. The dura was carefully removed using a 32G needle. Blood cells stained with SYTO62 (100 μl of 5 × 10^9 cells/ml) was then slowly injected through the retro-orbital route. Cortical venules with a diameter of <20 μm were chosen, the laser power was adjusted up to 300 mW, and imaged at 30 Hz to trace photoconversion of circulating cells. All animal experiments were performed in compliance with institutional guidelines and approved by the subcommittee on research animal care at the Harvard University and Massachusetts General Hospital.

3. Results and discussion

3.1 Theory of two-photon photoconversion

Photoconversion is mediated by electronic energy transition from absorbed photons. Thus, increasing incident optical power linearly accelerates the photoconversion speed. In a single-photon process, the conversion time (τ) is inversely proportional to irradiance (p) with units of [W/cm^2]:

$$\tau p = k^{(1)} \tag{2}$$

where $k^{(1)}$ is a single-photon conversion coefficient of a photoconverting molecule, which indicates the required fluence level for 1/e photoconversion. For one-photon photoconversion, fluence remains constant irrespective of the incident power. One of the fastest photoconvertible proteins, Dendra2, has $k^{(1)}$ of ~50 J/cm^2 [12]. The conversion rate ($1/\tau$) increases with the excitation power. However, in practice, the maximum optical intensity and fluence are limited by the risk of phototoxicity, which is typically mediated by photothermal and photochemical processes [18]. At a typical irradiance threshold of 10 W/cm^2, the conversion time is 5 s. This rather slow conversion speed has been a drawback for applications to fast dynamic processes such as cellular trafficking. Although there is a report on the conversion time of cells at 50 ms using Dendra2 [12], the irradiance used (10^3 W/cm^2) was about 100-fold higher than the reported photochemical cellular damage thresholds.

Two-photon processes provide a solution to overcome this limitation in conversion speed. First, near-infrared light, because of its lower photon energy, causes far less photochemical toxicity compared to visible and UV light. At a wavelength of 810 nm, the irradiance threshold for photochemical damage is ~10^3 W/cm^2, which is several orders-of-magnitude higher than those at UV-blue irradiation [19,20]. Second, as we will show below, the two-

Biomedical Optics EXPRESS

photon conversion process can be much faster than single-photon process for certain molecules.

The two-photon photoconversion time has an inverse quadratic dependence on the incident irradiance [21] (p):

$$\tau p^2 = k^{(2)} \tag{3}$$

where $k^{(2)}$ is a two-photon conversion coefficient of a molecule with units of [$W^2 \cdot s \cdot cm^{-4}$]. The total energy density required for two-photon photoconversion is inversely proportional to incident power, enabling faster conversion at lower overall fluence. This can be seen by substituting fluence into Eq. (3) to obtain:

$$k^{(1)} = k^{(2)} / p \tag{4}$$

To estimate two-photon photoconversion times using our technique, we derive the photoconversion time needed per focal spot for SYTO62, one of the fastest photoconverting cyanine dyes. Equation (3) can be re-written as:

$$\tau = \frac{k^{(2)}}{(I_p f \sigma)^2} \times \{duty\ \ cycle\} \tag{5}$$

where I_p is the peak irradiance with a unit of [$W \cdot cm^{-2}$], f is repetition rate at 80 MHz, σ is the pulse width at 150 fs, and duty cycle is defined as the two-photon excitation area divided by the total area scanned by the laser system [21]. Our empirically determined value of $k^{(2)}$ for SYTO62 is 1.48×10^{14} $W^2 \cdot s \cdot cm^{-4}$, which was obtained with a two-photon excitation area of 0.29 μm^2 (NA = 0.9, λ = 810 nm) and field of view of 300 × 300 μm^2 [22]. This gives an illumination duty cycle of 2.93×10^{-6}. Substituting these values into Eq. (5), we obtain:

$$\tau \cong \frac{3 \times 10^{18} J \cdot cm^{-2}}{I_p^2} \tag{6}$$

In two-photon processes, the maximum optical dosage is typically limited by nonlinear phototoxicity caused by instantaneous optical intensity [18,23,24] (I_p <10^{12} W/cm^2). Equation (6) shows that at the peak irradiance threshold of 10^{12} W/cm^2, the minimum photoconversion time per focal spot for SYTO62 is ~3 μs for a single focal volume. At this rate, the conversion for a single cell (typically ~80 μm^2 in area) takes <1 ms, which is over 5,000-times faster than the one-photon photoconversion time (5 s) of Dendra2. Other cyanine dyes, exhibiting faster kinetics [14], would offer shorter single-cell conversion times, for example 0.1 ms for SYTO61 and 0.2 ms for Cy5.5 (Table 1).

Biomedical Optics EXPRESS

Table 1. Single-cell conversion times for photoconvertible cyanine-based fluorophores (the area of the cell is assumed to be 80 μm^2).

Photoconvertible dye	Conversion time at NA = 0.9, λ = 810 nm
SYTO59	0.82 ms
SYTO61	0.097 ms
SYTO62	0.84 ms
SYTO80	4.0 ms
SYTO82	4.2 ms
SYTO84	2.4 ms
Alexa700	1.9 ms
Cyanine3.5 (Cy3.5)	0.73 ms
Cyanine5.5 (Cy5.5)	0.23 ms

3.2 Proof-of-principle experiments

We performed a photoconversion study on SYTO62 dye on a glass slide using a custom-built polygon-scanning two-photon system (Materials and Methods). To visualize both the unconverted (red) and converted (green) forms of SYTO62, we performed photoconversion on the central region of the sample using a circular aperture, while unconverted dye continuously diffuses into the periphery of this region (Fig. 1(a), Visualization 1).

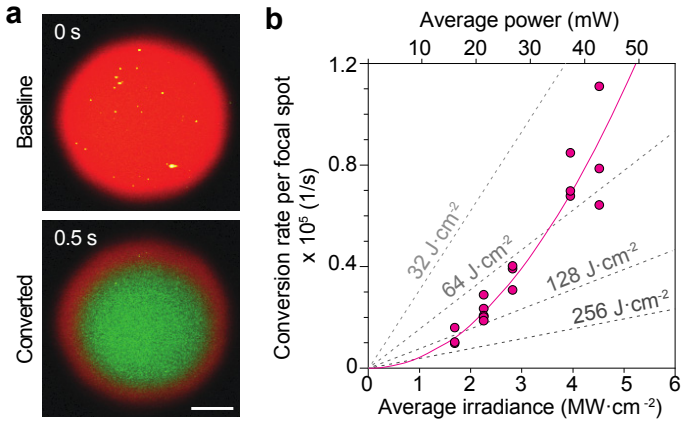

Fig. 1. Two-photon photoconversion kinetics of a SYTO62 dye. (**a**) Representative photoconversion of SYTO62 from red to green under two-photon excitation at 810 nm. The red ring around the converted area (lower image) is due to diffusion of the surrounding dye. (**b**) Quantification of conversion rate for different irradiance. The solid curve indicates the best-fit to a quadratic function and solid dashed lines indicate the equivalent-fluence lines.

As described previously [14], we observed a quadratic relationship between the irradiance and conversion speed as expected. Due to this non-linear relationship, faster photoconversion can be achieved at lower fluence levels using the same irradiance (Fig. 1(b)).

As shown in Table 1, cyanine-based dyes exhibit a variety of photoconversion kinetics owing to differences in their chemical structure [14,15]. Taking advantage of these differences, we demonstrated time-gated multiplexed labeling of cells (Fig. 2). We chose SYTO62 (red to green) and SYTO82 (green to blue) because of their ~5-fold difference in conversion rates at 810 nm. HeLa cells co-stained with SYTO62 and SYTO82 were first

Biomedical Optics EXPRESS

photoconverted from red to green after 3 s of full-field scanning (300 × 300 μm^2), which corresponds to ~2.7 ms exposure time per cell (cell area ≈80 μm^2). Continued irradiation results in photoconversion to blue at 15s of scanning, which corresponds to ~13 ms total exposure time per cell (Fig. 2(a)). We further found that at longer wavelengths (>800 nm), the photoconversion rate of SYTO82 drops significantly, while that of SYTO62 is relatively unchanged (Fig. 2(b)). This can be attributed to differences in their two-photon absorption spectra, given that the one-photon absorption maximum of SYTO62 (649 nm) is red-shifted compared to that of SYTO82 (541 nm).

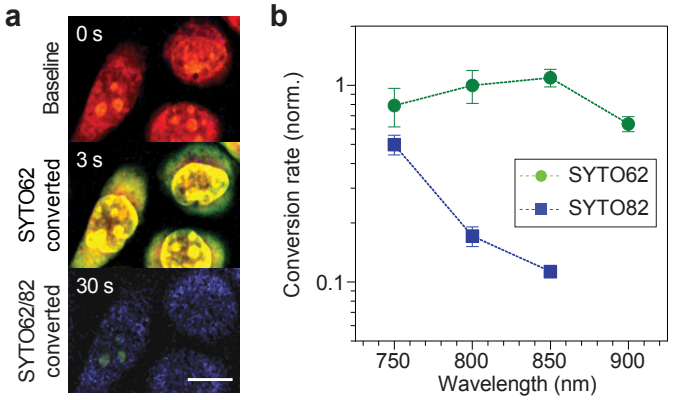

Fig. 2. Multiplexed photoconversion. (**a**) Multiplexed photoconversion of cultured HeLa cells stained with fast-converting SYTO62 (red to green) and slow-converting SYTO82 (red to blue). (**b**) Wavelength dependency of photoconversion rate.

3.3 Intracellular diffusion in axon fibers

We utilized our photoconversion technique to investigate intracellular diffusion kinetics in a live nerve fiber (Fig. 3). In a spinal axon stained with SYTO62, we photoconverted a ~10 μm-long segment of the axon and then traced the diffusion of the dye by time-lapse imaging (Materials and Methods). The optical intensity used for imaging was low enough to avoid any additional, measurable photoconversion. From the longitudinal diffusion profile of the dye, we calculated a diffusion coefficient of the photoconverted dye. The diffusion coefficient within the axon was measured to be ~3.93 × 10^{-9} cm^2·s^{-1}. To compare, we also measured the diffusion of SYTO62 in an artificial cerebrospinal fluid, and obtained a diffusion coefficient of ~4.25 × 10^{-6} cm^2·s^{-1}, 1,000 times faster than the dye diffusion in the neuron (Fig. 3(d)). We attribute the 1000-fold slower diffusion in the spinal axon to the compact subcellular structures, mainly composed of proteins and lipids [25], as well as binding of nucleic acids to the dye. This technique can be extended to multiplexed measurements of slow and fast diffusions by introducing multiple photoconvertible dyes (Fig. 2).

Biomedical Optics EXPRESS

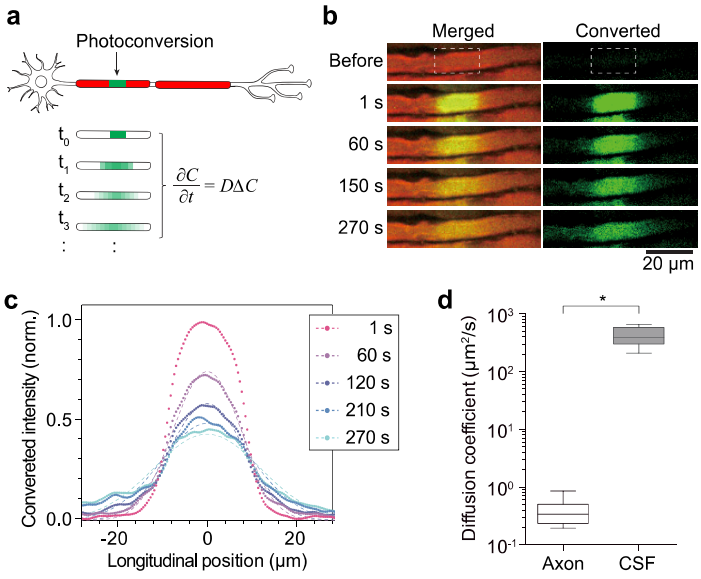

Fig. 3. Quantification of diffusion kinetics along axon fibers. (**a**) Schematic of the diffusion measurement along the axon fiber by photoconversion. (**b**) Representative time-series images of an axon before and after photoconversion. (**c**) Quantification of spatial profiles along the axon fibers over time. The dashed curves indicate the best-fit to the 1D diffusion equation (Eq. (1). (**d**) Measured diffusion coefficients from the axons and cerebrospinal fluid (CSF). *, $P < 0.001$.

3.4 Photoconversion of flowing cells in a microfluidic chip

We next applied our rapid photoconversion technique to flowing cells, which represents one of the fastest dynamic behaviors in biology. To mimic blood cells in circulation, we used a microfluidic chip perfused with mouse blood cells stained with SYTO62 (Fig. 4(a)). The flow rate was controlled by a syringe pump to be either ~0.2 mm/s, similar to the blood flow speed in venules, or ~3 mm/s, a typical blood flow speed in arterioles. With full-field scanning at 30 Hz, we observed that murine RBCs flowing at ~0.2 mm/s were fully converted within 1 s (Fig. 4(b) and Visualization 2). Since photoconversion only occurs when the focus of the scanned beam is within the target cell, line-scanning enhances the illumination efficiency over full-field scanning by reducing off-target illumination. By introducing the line-scanning at ~15 kHz along the direction of the flow, we successfully photoconverted RBCs flowing at arteriolar speeds (3.4 mm/s) with a conversion time of ~10 ms (Fig. 4(c)). For the simplicity of the analysis, we assumed that photoconversion occurs over the whole cell, considering the rotational motion of flowing RBCs and intracellular diffusion. To estimate whether the measured photoconversion time was consistent with theoretical prediction, we can re-write Eq. (6) as follows:

$$\tau_{cell} \cong \frac{3.7\times10^{18} J\cdot cm^{-2}}{I_p^2} \times \frac{cell\ area}{focal\ area} \tag{7}$$

Note that the constant in Eq. (6) differs from Eq. (5) since an objective of NA 0.8 was used for the microfluidic experiments. The 2P focal area for this objective was ~0.33 μm^2, while the average RBC area was measured to be ~13 μm^2. Here, τ_{cell} refers to the exposure time per cell or the duration for which a cell was actually illuminated. Experimentally, τ_{cell} was consistently sub-millisecond, independent of the scan type (e.g. 0.21 ms at 10^{12} W/cm^2), and about 50% higher than the predicted value (Fig. 4(d)). In Fig. 4(e), the apparent conversion

Biomedical Optics EXPRESS

time was plotted for blood cells of different sizes (white-blood cells and platelets). The conversion times were 0.1-1 s for full-field illumination and 2-10 ms for line-scan illumination. The predicted conversion times were calculated using the following relation:

$$\tau_{conversion} \cong \tau_{cell} \times \{illumination\ efficiency\} \quad (8)$$

For line-scanning, the illumination efficiency is the size of the cell (4 μm for RBC) divided by the scan length (150 μm in this case). For full-field scanning, the illumination efficiency is cell area (~13 μm^2) divided by the field-of-view (150 × 150 μm^2). As a result, line-scanning improves the illumination efficiency by a factor of ~50 in our-setup.

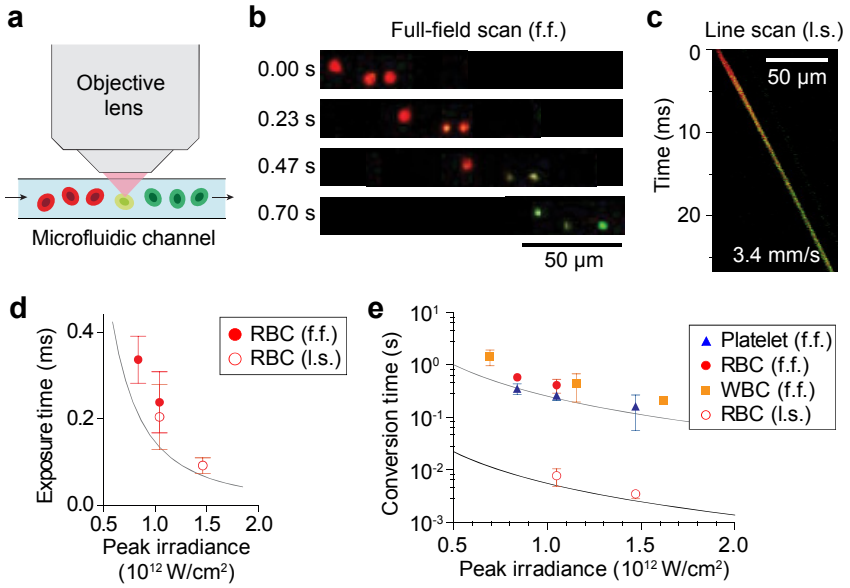

Fig. 4. Photoconversion of flowing cells in a microfluidic channel. (**a**) Schematic of photoconversion of flowing cells in a microfluidic channel. (**b**) Photoconversion of RBCs using full-field scanning. (**c**) Photoconversion of RBCs using a line-scan along the direction of flow. Cells flowing at 3.4 mm/s were photoconverted at 150 mW. (**d**) Photoconversion exposure time per RBC at 120, 150 and 210 mW, NA = 0.8. The line represents predicted exposure times based on previous spectroscopic data. f.f.: full-field scanning, l.s.: line-scanning. (**e**) Apparent conversion times for platelets, red blood cells (RBCs) and white blood cells (WBCs) plotted against peak laser irradiance. Lines represent predicted conversion times for full-field (f.f.) and line-scan (l.s.) methods.

At a peak irradiance of 10^{12} W/cm^2, our experimentally measured values for RBC full-field conversion (412 ms) was slightly larger than the predicted value (255 ms) from data measured of the dye only. This is likely due to geometric mismatch between the illumination beam and the cellular orientation, breaking the assumption of planar objects. As a result, apparent conversion times are increased by axial diffusion of unconverted dye into the laser focal plane. In comparison, our experimentally measured values for platelet full-field conversion (263 ms) are well matched with the predicted values, as expected given their smaller sizes (<2 μm).

3.5 Photoconversion of circulating cells in vivo

We next performed photoconversion of cells in blood circulation in a live mouse (Fig. 5(a)). Following intravenous administration of the SYTO62-stained blood cells, a venule in the brain cortex was imaged through a cranial window at a frame rate of 30 Hz. Using full-field scanning, we observed successful photoconversion in real-time for leukocytes, particularly

Biomedical Optics EXPRESS

those undergoing margination or rolling along the vessel wall (Fig. 5(b)-(d) and Visualization 3). Photoconversion was apparent in a second, which corresponds to an effective exposure time for the cell of ~0.3 ms. In this case, faster moving RBCs were not photoconverted due to insufficient exposure time. We envision that real-time feedback scanning of the conversion beam to track a target cell, for example via random access scanning [26], would enable photoconversion of a single cell within 1 ms using SYTO62. Even faster conversion rates may be achievable with Cy5.5 and SYTO61 (Table 1). Advanced scanless excitation methods, such as temporal focusing [27] or patterned excitation [28], would further improve the conversion speed especially for larger areas. In principle, several dyes could be used simultaneously to target cells flowing at different speeds (Fig. 2). Further chemical modification of cyanine-based dyes could provide new multiphoton photoconvertible dyes with more desirable characteristics, such as protein-specific labelling, faster kinetics or improved photostability.

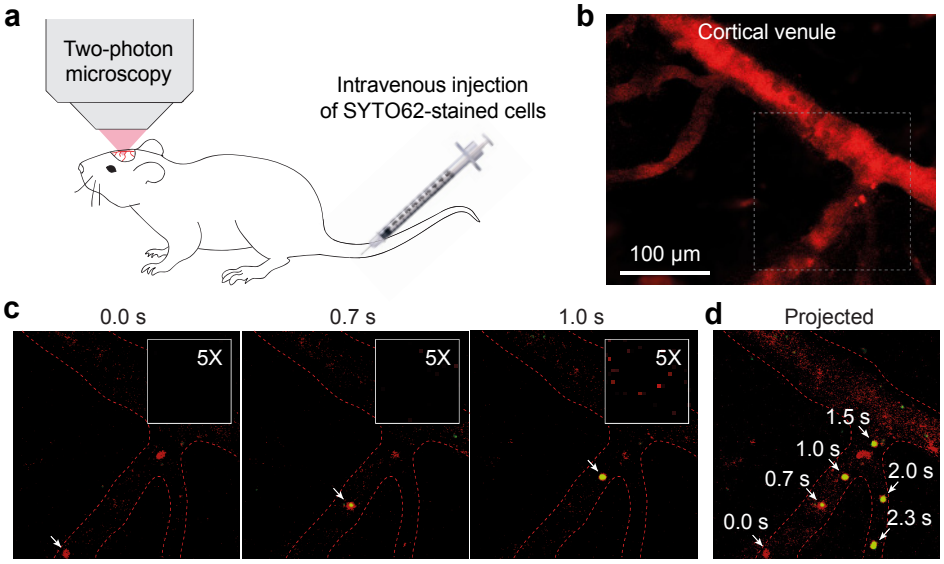

Fig. 5. Photoconversion of flowing cells *in vivo*. (**a**) Experimental scheme. An anesthetized mouse with a cranial window was intravenously injected with SYTO62 and studied under a two-photon microscopy. (**b**) A cortical vasculature imaged by two-photon fluorescence of SYTO62. Dotted white box is the cortical venue where photoconversion was observed. (**c**) Time-lapse images of photoconversion of a flowing WBC (indicated by an arrow) *in vivo*. Inset shows magnified image of the WBC. (**d**) A merged image showing leukocyte trajectory for annotated time points.

4. Conclusion

Using a Ti:Sapphire laser at intensities below photodamage thresholds, we have achieved successful photoconversion of various cyanine-based, commercial dyes. The photoconversion speed was less than one millisecond exposure time per cell, faster than any previously reported process. Two-photon photoconversion of cyanine-based fluorophores is well suited for rapid *in situ* labeling of cells. Harnessing the rapid photoconversion kinetics of SYTO62, we demonstrated several biological applications, including pulse-chase measurement of intracellular diffusion kinetics and *in situ* labeling of flowing cells in a microfluidic channel, and cells in circulation *in vivo*.

Funding

Human Frontier Science and Foundation (RGP0034/2016); the National Institutes of Health (P01-HL120839); Korea Institute of Science and Technology (Grant); the Institute of Basic

Biomedical Optics EXPRESS

Science (IBS-R015-D1); and by the Basic Science Research Program through the National Research Foundation of Korea (NRF), funded by the Ministry of Education (2017R1A6A1A03015642).

Disclosures

The authors declare that there are no conflicts of interest related to this article.